Co-published by
Institute of Fluid-Flow Machinery
Polish Academy of Sciences
Committee on Thermodynamics and Combustion
Polish Academy of Sciences

http://www.imp.gda.pl/archives-of-thermodynamics/

Shape effects on steady flow and heat transfer of Cu-nanofluid over a nonlinear stretching surface with Joule heating

Ramzan Ali[a*], Ainura Mitalipova[b], Syed Wajeeh Ul Hussan[c], Abdikerim Kurbanaliev[b], Azeem Shahzad[c], Mukhammadmuso Abduzhabbarov[d]

[a]University of Doha for Science and Technology, 68 Al Tarafa, Jelaiah Street, Duhail North, 24449, Doha, Qatar
[b]Osh State University Kyrgyz Republic, Lenina Street 331, 714000, Kyrgyzstan
[c]University of Engineering and Technology, Department of Mathematics, Faculty of Basic Sciences, Taxila, HMC Link Rd, Taxila, 47050, Pakistan
[d]Westminster International University in Tashkent, School of Law, Technology & Education, Istiqbol 12, Tashkent, 100047, Uzbekistan
*Corresponding author email: ramzan.ali@udst.edu.qa

Received: 03.07.2024; revised: 22.05.2025; accepted: 27.05.2025

Abstract

Nanofluids have garnered significant interest in various fields due to their numerous advantages and potential applications. The appeal of ethylene glycol (EG)-based Cu-nanofluid lies in its excellent thermal conductivity, stability, and ability to enhance heat transfer properties, making it a promising candidate for diverse industrial applications. In this study, we analyse the flow behaviour of EG-based copper (Cu) nanofluid over a nonlinear stretching surface under the influence of Joule heating effects. The research involves the development of a mathematical model and formulating of governing equations represented as system of partial differential equations, which are subsequently transformed into nonlinear ordinary differential equations through suitable transformations. A numerical framework based on MATLAB bvp4c solver technique is employed to obtain approximate solutions. The study examines the influence of dimensionless parameters on velocity and thermal distributions. The findings for the local Nusselt number and skin friction are presented in tabular form, highlighting the effects of key parameters. The results are benchmarked against three different sources from existing literature, showing strong agreement in the case of reduced Nusselt number.

Keywords: Joule heating; MHD flow; Cu-nanofluid; Stretching surface

Vol. 46(2025), No. 3, 89–104; doi: 10.24425/ather.2025.156581

Cite this manuscript as: Ali, R., Mitalipova, A., Ul Hussan, S.W., Kurbanaliev, A., Shahzad, A., & Abduzhabbarov, M. (2025). Shape effects on steady flow and heat transfer of Cu-nanofluid over a nonlinear stretching surface with Joule heating. *Archives of Thermodynamics*, 46(3), 89–104.

1. Introduction

Nanofluids are stable dispersions of nanoparticles in a base fluid, in which the thermophysical properties, such as thermal conductivity, are enhanced several times compared to those of the pure liquid. On the other hand, these nanofluids are used in various sectors such as heat transfer, lubrication, biomedicine, and solar panels to have better optical characteristics and absorption ability of CO_2. Although nanofluids have many advantages over other types of fluids, their stability is still a major hurdle when using them in diverse engineering fields. To overcome the issue, different stabilization strategies combined with numerous performance evaluation approaches have been introduced. It is

Nomenclature

A – proportionality constant
$\boldsymbol{B}$ – magnetic field, T
B_0 – constant magnetic field, T
c – dimensional constant
C_p – specific heat capacity, (J/kg K)
Ec – Eckert number
$f'(\eta)$– dimensional velocity distribution
$\boldsymbol{J}$ – current density vector, A/m^2
k – thermal conductivity, W/(m K)
K – slip parameter
$\boldsymbol{L}$ – velocity gradient tensor, 1/s
m – shape factor
n – stretching parameter
M – magnetic parameter
Nu – Nusselt number
Pr – Prandtl number
$\boldsymbol{q}$ – electric charge, C
Re – Reynolds number
T – temperature parameter, K
u, v– velocity components in the x- and y-axis directions, m/s
U – surface velocity, m/s
$\boldsymbol{V}$ – velocity vector, m/s
x, y – Cartesian coordinates, m

Greek symbols

α – thermal diffusivity, m^2/s
ε_i – constants (i = 1,2,3,4,5)
η – similarity variable
$\theta(\eta)$– dimensionless temperature distribution
μ – dynamic viscosity, Pa·s
υ – kinematic viscosity, m^2/s
ρ – density, kg/m^3
σ – electrical conductivity, S/m
ϕ – volume fraction

Subscripts and Superscripts

f – fluid
nf – nanofluid
s – solid particles
w – wall
∞ – surrounding fluid
$(\cdot)'$, $(\cdot)''$, $(\cdot)'''$ – differentiation with respect to η

Abbreviations and Acronyms

EG – ethylene glycol
MHD– magnetohydrodynamics
ODE – ordinary differential equation
PDE – partial differential equation

generally accepted that the nanoparticle and base fluid characteristics, preparation methods, external factors and stabilizer content play critical roles in assessing nanofluid stability over time.

Literature review reveals that nanofluids are a rapidly growing field of research that is currently applied in many different fields. Several attempts have been made simultaneously to create stable nanofluids.

Copper (Cu) nanofluid can be defined as a liquid that comprises copper nanoparticles suspended in the base fluid, which can be, among others, water, ethylene glycol, or oil. The following properties of copper are some of the reasons why copper nanofluids are applied in heat exchangers, solar collectors, cooling of electronic devices, and some other loads where the process of heat transfer needs improvement, high thermal conductivity and electrical conductivity. This is because the conduction of the copper within the nanofluids is high, hence improving the energy and overall performance of the nanofluids. Copper is also less expensive to incorporate into other nanomaterials and other related compounding materials to which it can be added. Copper nanoparticles are also known to have an antimicrobial property that makes these fluids useful in reducing biofouling in systems where water is used as the heat transfer medium. Hence, copper is employed in nanofluids due to its thermal/electrical conductivity, reasonable cost, and bacteriostatic properties. Eastman et al. [1] investigated that the nanofluid of copper nanoparticles in ethylene glycol has significantly higher effective thermal conductivity than pure or oxide nanoparticles. This increase can be up to 40%, contradicting previous predictions of particle shape and size having no effect on thermal conductivity. Chakraborty and Panigrahi [2] discussed the stability of nanofluid and its significance in industrial applications, and offer recommendations for its wider practical adoption. Patel et al. [3] explored thermal conductivities of nanoparticles in water and toluene media, revealing variations based on particle type and stabilization, with additional factors influencing the thermal conductivity mechanism in nanofluids. Liu et al. [4] examined the flow and heat transfer near a rotating disk containing nanofluids, showing variations in boundary layer thicknesses and heat transfer rates with different nanoparticle volume fractions and materials. The flow and heat transfer properties of nanofluids in a rotating frame were studied by Das [5], who considered two types of nanofluids and analysed the effects of different parameters. Nanofluid flow and heat transfer are extensively studied for various industrial and engineering applications.

Utilizing the Buongiorno model, the work [6] investigates mass and heat transfer in nanofluid-connected flow and discovers that heat transmission diminishes as thermal radiation and convection parameters grow. Research [7] explores the impact of external forces like natural convection, thermal radiation, and chemical reactions on heat and mass transfer. Nanofluid combinations can minimize the skin friction coefficient and maximize heat transfer rates. Magnetic fields and thermal radiation influence hybrid nanofluids, enhancing thermal conductivity. The study of Sakiadis [8] offers valuable insights into optimizing nanofluid flow and heat transfer processes. Ferdows et al. [9] analysed the effects of MHD flow and Hall currents on boundary layer flow over a three-dimensional extending surface to demonstrate improvements in velocity, profile and heat flux, and transfer rates.

Ahmad et al. [10] examined the mixed convection flow of hybrid nanofluid over a nonlinear stretching sheet, showing that the magnetic field velocity decreases and thermal radiation temperature increases. The influence of a magnetic field and nano-

particles on Carreau fluid flow and heat, and mass transfer over a porous nonlinear stretching surface was studied by Eid et al. [11]. Hayat et al. [12] present a numerical simulation study on boundary layer flow over a nonlinear curved stretchable surface, examining various parameters. Zaimi et al. [13] present a mathematical study on boundary layer flow and heat transfer in a nanofluid, examining the effects of parameters and identifying dual solutions. When dust particles and polymers combine in a viscous liquid, Athar et al. [14] observed that the polymers undergo deformation inside the boundary layer but not outside of it. Shah et al. [15] used graphs and the homotopy analysis approach to analyse the heat transfer and boundary layer flow of couple stress fluid at the stagnation point over an exponentially extending surface.

Venkateswarlu et al. [16] and Vidya et al. [17] conducted a study on the incompressible stagnation point flow of a conductive hyperbolic radiative nanoliquid past a stretching surface. They found that increasing Weissenberg's number reduced fluid velocity. Hashim et al. [18] extended the mathematical formulation for the aligned magnetic field on Williamson fluid over a stretching sheet with Newtonian heating, analysing the effects of various parameters on temperature and velocity profiles.

Chen [19] examined both Joule heating and viscous dissipation on MHD (magnetohydrodynamic) flow over a stretching sheet, considering the influence of free convection, thermal radiation, and surface suction/blowing. The study of Khashi'ie et al. [20] reveal the variation of flow and heat transfer characteristics of a hybrid nanofluid of a shrinking cylinder with Joule heating with distinct types of nanofluids. Joule heating effects on fluid movement and heat transmission over an exponentially extending sheet are explored by Srinivasacharya and Jagadeeshwar [21] mainly in view of its relevance to industrial applications and magnetohydrodynamic flows. Ganesh Kumar et al. [22] discuss the effect of viscous dissipation and Joule heating on Jeffrey nanofluid and how the temperature profile and the thickness of the thermal boundary layer are affected by it. Ghaffarpasand [23] investigates MHD natural convection in a cavity filled with Fe_3O_4-water nanofluid, revealing improved heat transfer with ferrite nanoparticles and increased entropy generation under Joule heating and Lorenz force. Mutuku et al. [24] analyse the impact of Joule heating and viscous dissipation on nanofluid flow past an inclined plate, highlighting the significant influence of controlling parameters on flow fields. Ali et al. [25] conducted a study on the impact of various forces and parameters on ethylene glycol-based nanofluids suspended above a thin vertical needle.

Shankar Goud et al. [26] investigated the effects of Joule heating on surfaces that stretch exponentially, and Khashi'ie et al. [27] communicated about the Joule heating effect of hybrid nanofluid. According to the research of Rana et al. [28] on an exponentially stretched surface, the thermal boundary layer structure is improved by both Joule and viscous heating mechanisms, which lowers nano-liquid velocity. Viscoelastic nanofluid has greater momentum, according to research by Tarakaramu et al. [29] on the effects of different physical parameters on MHD nanofluid flow to a stretched surface.

The research community in engineering and modelling has extensively investigated the boundary layer flow and heat transfer of nanofluids under Joule heating, focusing on factors like hydromagnetic forces, mixed convection, thermal stratification, chemical reactions, and viscous dissipation. Saleem et al. [30] investigated the impact of various copper nanoparticle shapes on the flow and heat transfer characteristics of a water-based nanofluid over a flat surface. Fakour et al. [31] studied the flow and heat transfer characteristics of nanofluid thin films over an unsteady stretching elastic sheet using the lattice Boltzmann method (LBM). Using aluminum and copper with water, Mathews and Tallab [32] discussed the nonlinearity of the stretching sheet. Triveni et al. [33] analyse the heat transfer of MHD Casson nanofluid flow over a nonlinear stretching sheet in the presence of a nonuniform heat source. Hayat et al. [34] analysed MHD thin film flow with viscous dissipation and slip effects for nanofluids of various nanoparticle shapes on an unsteady radially stretching surface.

A numerical study using a vertical cone and Williamson nanofluid flow has been discussed by Sathyanarayana and Goud [35]. Joachimiak et al. [36] investigated the effects of different physical criteria on thermochemical attitudes while conducting a numerical study of an aluminum alloy. In his discussion of the various nanoparticle shape parameters, Hayat and Shahzad [37] included a numerical study and analysis of the impacts of heat transmission and thin film flow for various gold nanoparticle shapes on a vertically stretched sheet. In another study [38], authors considered gold nanoparticles and the effects of different shape factors on a radial stretching sheet. Ali et al. [39] proposed a model for the unsteady flow of silica nanofluid over a stretching cylinder and considered the shape effects of the nanoparticles. Gangadhar et al. [40] investigated the flow performance of silver-engine oil-based nanofluids with different non-Newtonian models through a Riga plate. In [41], Gangadhar and coauthors presented a numerical study on the performance of an HVAC (heating, ventilation, and air conditioning) system utilizing Sutterby flow ternary nanofluids, with a focus on a Cu-Ag-AA7075/$C_6H_9NaO_7$ nanofluid. In other works [42−44], Gangadhar et al. provided the PDEs (partial differential equations) model-based Williamson fluid over a heated cylinder with convective heating. Furthermore, they considered thermal radiation and Cattaneo-Christov energy diffusion. They incorporated graphene and magnetic oxide nanoparticles to improve thermal conductivity. Their studies showed that enhanced thermal radiation increases the temperature of the fluid, while suction reduces skin friction coefficients but enhances heat and mass transfer rates. Their model was validated by comparing results with existing literature. Furthermore, Gangadhar et al. [45] explored the self-propelled movement of gyrotactic swimming microorganisms in a Casson nanofluid slip flow over a stretching cylinder with a strong magnetic field, using a non-dimensional numerical model and bvp4c technique. In another work [46], Gangadhar et al. examined the effect of a strong magnetic field and thermal radiation on the free convective flow of a ternary nanofluid over a moving wedge surface.

The PDE model provided in the manuscript has potential applications in heat transfer enhancement. It is evident that the copper-based nanofluid has extraordinary thermal conductivity.

This peculiar property makes them an ideal candidate for enhancing heat transfer for real-life applications, including cooling microelectronics and solar collectors. The proposed model, which includes PDEs with complex boundary conditions and the study of different particle shapes, is the first of its kind. Nanofluidic models with nonlinear stretching surfaces are highly applicable in industrial processes like sheet drawing, sustainable polymer production. The literature suggests studying efficient cooling and uniform heat distribution for high-quality engineering products. Nanofluid models are used for controlled heating processes in aerospace, automation and renewable energy. A better PDE model with realistic boundary conditions will enable the research community to design efficient devices.

This article investigates the steady heat transfer and flow in Cu nanoparticles with the added effects of thermal radiation, Joule heating, magnetohydrodynamics, and velocity slip over time-independent nonlinear stretching surfaces. It is the first study to investigate steady-state heat transfer and flow over a time-independent stretching surface with ethylene glycol (EG) as the base liquid. Here, we utilize a Cartesian coordinate system for the mathematical description of the problem and solve the obtained system of simplified nonlinear ordinary differential equations (ODEs) by utilizing an effective and convergent technique bvp4c. All the necessary calculations are performed in MATLAB. Additionally, a graph is included to explain the impact of physical parameters on temperature, velocity, skin friction number and Nusselt number.

2. Materials and methods

Heat and mass transfer analysis of a steady, viscous, incompressible nanofluid under laminar flow through a stacking and two-dimensional, regulated, nonlinear and stretching surface is depicted in Fig. 1. Parameter T_w represents the surface temperature and T_∞ denotes the temperature of the surrounding fluid. The *x*-axis is taken along the surface and the *y*-axis is taken perpendicular to it.

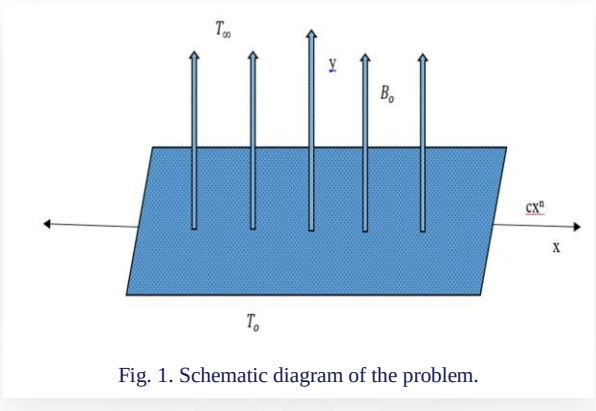

Fig. 1. Schematic diagram of the problem.

It is further assumed that the stretching velocity of the surface is given by

$$U = cx^n, \tag{1}$$

where *n* is the stretching parameter, and the magnetic field applied perpendicular to the surface is equal to

$$\boldsymbol{B} = B_0 x^{\frac{n-1}{2}}, \tag{2}$$

where B_0 is a constant magnetic field. It was also assumed that any generated magnetic field component is much smaller than the external magnetic field and the base fluid is ethylene glycol containing copper nanoparticles. These nanoparticles exist in various shapes and have a uniform size without any distortions, remaining in thermodynamic equilibrium with the fluid in which they are suspended.

In light of the above assumptions, the governing equations of continuity, momentum and energy for the current study are expressed as follows:

$$\nabla \cdot \boldsymbol{V} = 0, \tag{3}$$

$$\rho_{nf}(\boldsymbol{V} \cdot \nabla)\boldsymbol{V} = \nabla \cdot \boldsymbol{\tau} + \boldsymbol{J} \times \boldsymbol{B}, \tag{4}$$

$$\rho_{nf}\frac{dT}{dt} = \boldsymbol{\tau} \cdot \boldsymbol{L} - \nabla \cdot \boldsymbol{q} + \frac{J^2}{\sigma_{nf}}, \tag{5}$$

where $\boldsymbol{V}$ is the velocity vector, $\boldsymbol{\tau}$ is the stress tensor, $\boldsymbol{J}$ is the current density vector, T is the temperature, t is the time, ρ_{nf} is the density of the nanofluid, $\boldsymbol{L}$ is the velocity gradient tensor, $\boldsymbol{q}$ is the electric charge of particles. In the case of a two-dimensional nanofluid model, the vector form reduces to the following system of equations [39,40]:

$$\frac{\partial u}{\partial x} + \frac{\partial v}{\partial y} = 0, \tag{6}$$

$$\left(u\frac{\partial u}{\partial x} + v\frac{\partial u}{\partial y}\right) = \frac{\mu_{nf}}{\rho_{nf}}\left(\frac{\partial^2 u}{\partial y^2}\right) - \frac{\sigma_{nf}B^2}{\rho_{nf}}u, \tag{7}$$

$$\left(u\frac{\partial T}{\partial x} + v\frac{\partial T}{\partial y}\right) = \alpha_{nf}\frac{\partial^2 T}{\partial y^2} + \frac{\mu_{nf}}{(\rho C_p)_{nf}}\left(\frac{\partial u}{\partial y}\right)^2 + \frac{\sigma_{nf}B^2}{(\rho C_p)_{nf}}u^2, \tag{8}$$

where μ_{nf} is the dynamic viscosity of the nanofluid and α_{nf} is the thermal diffusivity of the nanofluid, *B* is the strength of the magnetic field and C_p is the specific heat.

The boundary conditions for the problem under consideration at $y = 0$ are:

$$\begin{cases} u = U + A\,\nu_f\dfrac{\partial u}{\partial y}, \\ v = 0, \\ T = T_w, \end{cases} \tag{9}$$

as $y \to \infty$, u approaches 0 and T approaches T_∞.

The pertinent physical parameters from literature are defined as [31]:

$$\begin{gathered} \alpha_{nf} = \frac{k_{nf}}{(\rho C_p)_{nf}}, \\ \rho_{nf} = (1-\phi)\rho_f + \phi\rho_s, \\ \mu_{nf} = \mu_f(1 + A_1\phi + A_2\phi^2), \\ \sigma_{nf} = \sigma_f(1-\phi)\sigma_f + \phi\sigma_s, \end{gathered} \tag{10}$$

$$\left(\rho C_p\right)_{nf} = (1-\phi)\left(\rho C_p\right)_f + \phi\left(\rho C_p\right)_s,$$

$$\frac{K_{nf}}{K_f} = \left[\frac{K_s + (m-1)K_f + (m-1)\left(K_s - K_f\right)\phi}{K_s + (m-1)K_f - \left(K_s - K_f\right)\phi}\right]$$

where ϕ is the volume fraction, m is the shape factor, K_{nf}, K_f, and K_s are slip parameters of nanofluid, base fluid and solid particles, respectively.

Using the similarity transformation [30] mentioned below, we will obtain the dimensionless form of the governing equations:

$$\begin{aligned} \psi &= \mathrm{e}^{-\frac{1}{2}} f(\eta), \\ \eta &= \frac{y}{x}\mathrm{Re}^{\frac{1}{2}}, \\ \theta(\eta) &= \frac{T - T_\infty}{T_w - T_\infty}, \end{aligned} \tag{11}$$

where ψ is the stream function, η is the similarity variable, and θ is the dimensionless temperature. Function f represents a dimensionless similarity function that describes the velocity distribution within the boundary layer. The pattern of flow is defined by the stream function, and the components of velocity can be obtained as follows:

$$\begin{aligned} u &= \frac{\partial \psi}{\partial y} \\ v &= -\frac{\partial \psi}{\partial x} \end{aligned} \tag{12}$$

Here

$$\mathrm{Re} = \frac{xU}{\vartheta_f} \tag{13}$$

is the Reynolds number. From the above transformation, we have

$$\begin{aligned} u &= Uf(\eta), \\ v &= -U\mathrm{Re}^{\frac{1}{2}}\left[\tfrac{n+1}{2} f(\eta) + \tfrac{n-1}{2}\eta f'(\eta)\right]. \end{aligned} \tag{14}$$

By using the above transformation, the continuity Eq. (6) holds automatically, and Eqs. (7) and (8) take the following non-dimensional forms, respectively:

$$\begin{aligned} \varepsilon_1 f''' - n f'^2 - \frac{n+1}{2} f f'' - \varepsilon_3 M f' \\ - (n-1)\,\eta f' f'' = 0, \end{aligned} \tag{15}$$

$$\begin{aligned} \theta''(\eta) + \frac{\mathrm{Pr}}{\varepsilon_2}\Big(\frac{n+1}{2} f\theta'(\eta) + \varepsilon_4 \mathrm{Ec} f''^2 \\ + \varepsilon_5 \mathrm{Ec}\, M f'^2\Big) = 0. \end{aligned} \tag{16}$$

Now, the boundary conditions in terms of the transformed variable become:

$$\begin{cases} f(0) = 0, \\ f'(0) = 1 + Kf''(0), \\ f'(\infty) = 0, \\ \theta(0) = 1, \\ \theta(\infty) = 0. \end{cases} \tag{17}$$

The dimensionless constants are defined as follows:

Prandtl number $\quad \mathrm{Pr} = \frac{\left(\rho C_p \nu\right)_f}{kf},$

slip parameter $\quad K = A\sqrt{\frac{\nu\, U_w}{x}},$

Eckert number $\quad \mathrm{Ec} = \frac{U^2}{C_p(T_w - T_\infty)},$

magnetic parameter $\quad M = \frac{B_0^2\, \sigma_f}{c\, \rho_{nf}}.$

Since the Nusselt number (Nu) and skin friction coefficient (C_f) are significant in engineering, they can be defined as:

$$\begin{aligned} C_f &= \frac{T_w}{\rho_f U^2}, \\ \mathrm{Nu} &= \frac{x\, q_w}{k_f(T_w - T_\infty)}. \end{aligned} \tag{18}$$

Further the constants ε_i, for $i = 1, \ldots, 5$ are defined as:

$$\begin{aligned} \varepsilon_1 &= \frac{1 + A_1\phi + A_2\phi^2}{1 - \phi + \phi\left(\frac{\rho_s}{\rho_f}\right)}, \\ \varepsilon_2 &= \frac{\frac{K_{nf}}{K_f}}{1 - \phi + \phi\left[\frac{(\rho C_p)_s}{(\rho C_p)_f}\right]}, \\ \varepsilon_3 &= \frac{1 - \phi + \phi\left(\frac{\sigma_s}{\sigma_f}\right)}{1 - \phi + \phi\left(\frac{\rho_s}{\rho_f}\right)}, \\ \varepsilon_4 &= \frac{1 + A_1\phi + A_2\phi^2}{1 - \phi + \phi\left[\frac{(\rho C_p)_s}{(\rho C_p)_f}\right]}, \\ \varepsilon_5 &= \frac{1 - \phi + \phi\left(\frac{\sigma_s}{\sigma_f}\right)}{1 - \phi + \phi\left[\frac{(\rho C_p)_s}{(\rho C_p)_f}\right]}. \end{aligned} \tag{19}$$

3. Numerical solution

This article uses the bvp4c [31] in MATLAB to get the mathematical solution of the reduced Eqs. (15) and (16) along with the boundary conditions Eq. (17). The main characteristics of the suggested bvp4c technique, which include handling single boundary value problems (BVPs), direct acceptance of both

two-point and multipoint BVPs with improved accuracy, and faster convergence with reduced error, are well recognized in the research community. The basic numerical method implemented in bvp4c is a form of Simpson's method that is rather generic and can be found in numerous programs. To apply this strategy, the third-order ODE (15) and the second-order ODE (16) are transformed into the first-order differential equations as follows:

$$f = y_{(1)}. \tag{20}$$

Then we can write

$$f' = y'_{(1)} = y_{(2)},$$

$$f'' = y'_{(2)} = y_{(3)},$$

$$f''' = y'_{(3)} = \frac{1}{\varepsilon_1}\left(n y_{(2)}^2 + \frac{n+1}{2} y_{(1)} y_{(3)} + \varepsilon_3 M y_{(2)} + n\eta y_{(2)} y_{(3)}\right), \tag{21}$$

$$\theta = y_{(4)},$$

$$\theta' = y'_{(4)} = y_{(5)},$$

$$\theta'' = y'_{(5)} = \frac{\mathrm{Pr}}{\varepsilon_2}\left[-\left(\frac{n+1}{2}\right) y_{(1)}\, y_{(5)} - \mathrm{Ec}\, \varepsilon_4 y_{(3)}^2 - \varepsilon_5\, \mathrm{Ec}\, M y_{(2)}^2\right].$$

Boundary conditions are:

$$\begin{cases} y_{(2)}(0) = 1 + K y_{(3)}(0), \\ y_{(1)}(0) = 0, \\ y_{(2)}(\infty) = 0, \\ y_{(4)}(\infty) = 0. \end{cases} \tag{22}$$

4. Results and discussion

In this research, we explore a model that investigates how nanofluids, containing copper nanoparticles of various shapes, behave in two-dimensional boundary layer flow. By employing similarity transformations, we transform the given differential equations into simpler ordinary differential equations. Afterward, we analyse how factors like the magnetic parameter, slip parameter, volume fraction, stretching parameter and Eckert number impact the velocity and temperature profiles within the layer, considering various shapes of copper nanoparticles. These influences are illustrated through graphs shown in Figs. 2 to 12.

The pertinent impact of the magnetic parameter, which occurs through the modelling of Maxwell's equations on the velocity profile within the boundary layer, is comprehensively analysed and illustrated in Fig. 2 for EG-Cu nanofluid for various nanoparticle shapes. The results are presented for blade, brick, cylinder, platelets, and sphere, highlighting the influence of the shape factor on the velocity profile. Increasing the magnetic parameter leads to a noticeable reduction in the velocity of copper

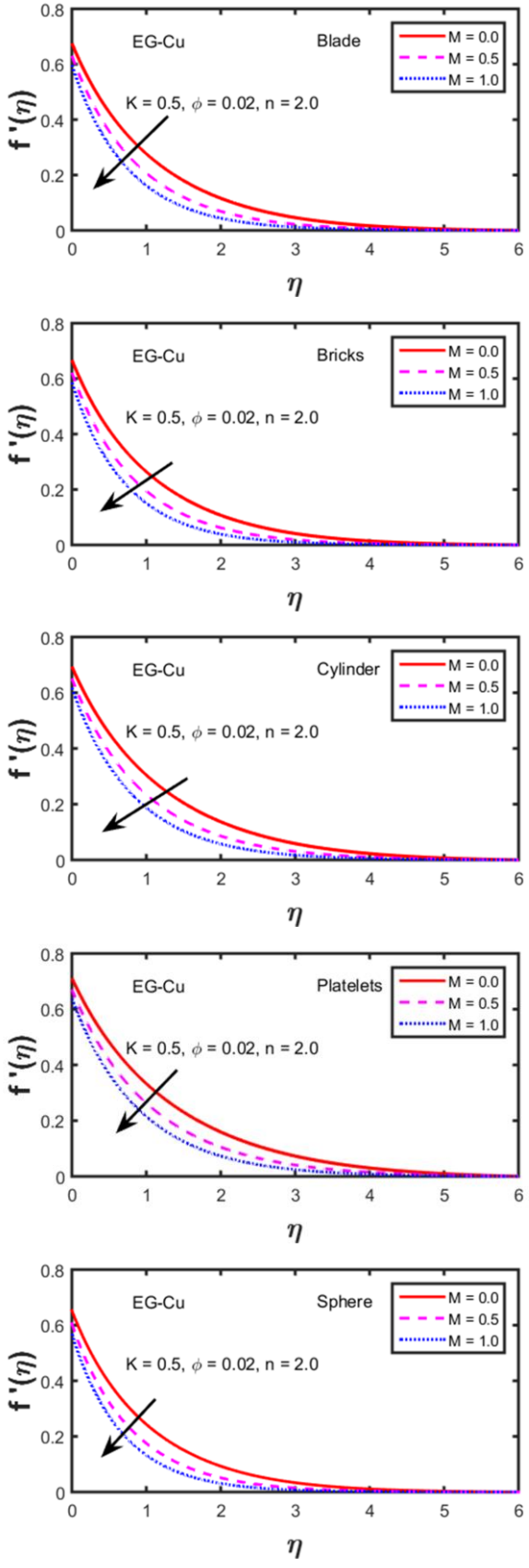

Fig. 2. Impact of the magnetic parameter (M) on the velocity profile of EG-Cu nanofluid for various nanoparticle shapes: blade, brick, cylinder, platelets, and sphere.

nanofluids across various nanoparticle shapes. This effect is attributed to the enhancement of Lorentz forces, which act as resistive forces opposing the fluid's motion, thereby decreasing the velocity profile.

From the graphical representation of the velocity profile, it is clear that an increase in the magnetic parameter (M) leads to a noticeable reduction in the velocity of the copper nanofluid across all nanoparticle shapes. This peculiar behaviour can be attributed to the presence of the Lorentz force, which arises from the interaction between the externally applied magnetic field and the induced electrical currents within the nanofluid. The Lorentz force acts as a resistive drag force, opposing the motion of the fluid and thereby reducing its velocity profile.

This effect is particularly significant within the boundary layer, where the interplay between magnetic forces and viscous forces becomes more pronounced. The reduction in velocity due to the magnetic parameter highlights the potential for controlling fluid dynamics in magnetohydrodynamic applications, where the magnetic field is utilized to manipulate the flow properties of conducting fluids, such as nanofluids, for engineering and industrial purposes.

Figure 3 presents the relationship between the magnetic parameter M and the fluid temperature of EG–Cu nanofluid for different nanoparticle shapes, including blade, brick, cylinder, platelets and sphere. The results clearly demonstrate that fluid temperature increases as M rises, emphasizing the critical role of nanoparticle geometry in dictating thermal behaviour. This trend is explained by the Lorentz force, which is induced when a magnetic field interacts with an electrically conducting nanofluid. The Lorentz force resists the motion of nanofluid particles, thereby dissipating their kinetic energy and converting it into thermal energy. This process enhances the overall heat transfer rate of the fluid. Importantly, the results highlight a dual effect: while the Lorentz force restricts particle movement and slows fluid motion, it simultaneously boosts thermal energy generation through dissipation. Consequently, higher values of M lead to a substantial rise in fluid temperature, as depicted in Fig. 3. These observations underscore not only the impact of magnetic fields on thermal transport but also the significance of nanoparticle shape in modifying velocity and temperature distributions within nanofluids.

Figure 4 illustrates the influence of the slip parameter K on the velocity profile of EG–Cu nanofluid for various nanoparticle shapes. As K increases, the velocity decreases for all particle geometries due to reduced momentum transfer at the fluid–wall interface under partial slip conditions. The results also highlight that nanoparticle shape strongly influences this behaviour: particles with larger surface areas, such as blades or platelets, exhibit more pronounced velocity reductions, while smoother geometries, like spheres, show smaller variations. These observations emphasize the importance of nanoparticle shape in governing flow characteristics under slip conditions.

Figure 5 depicts the influence of the partial slip condition (K) on the thermal field in EG-Cu nanofluid for five distinct nanoparticle shapes: blade, brick, cylinder, platelets, and sphere.

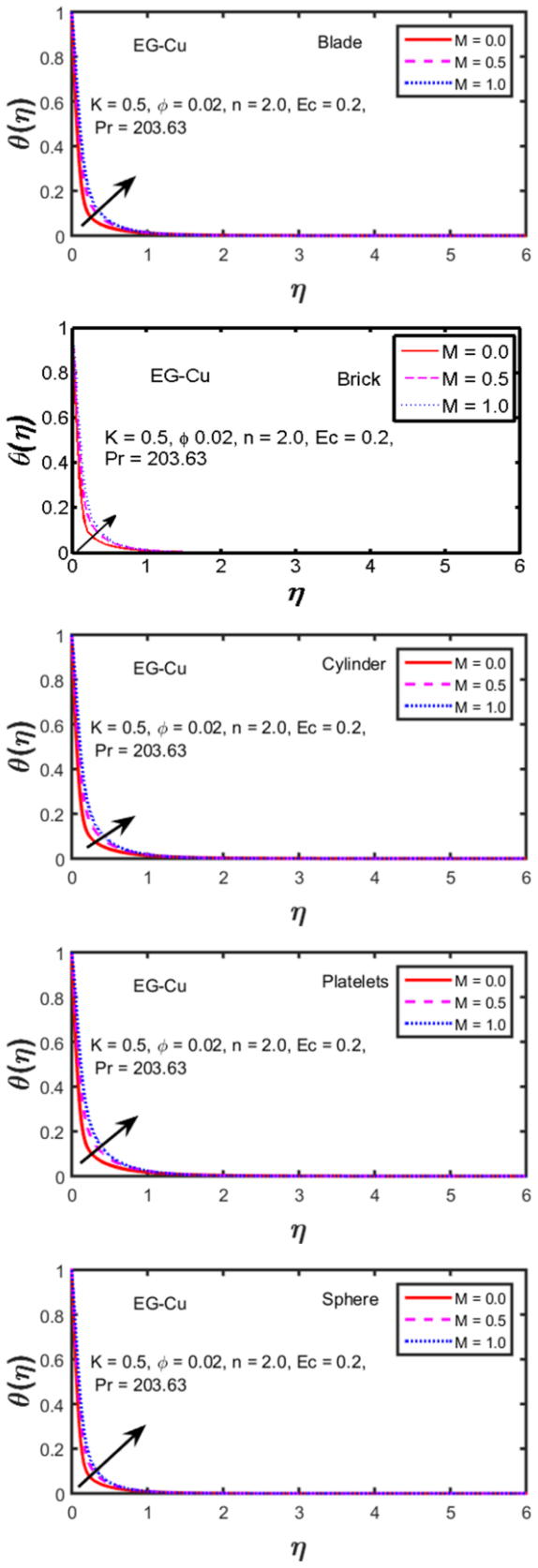

Fig. 3. Influence of magnetic parameter (M) on temperature profile of EG-Cu nanofluid for various nanoparticle shapes: blade, brick, cylinder, platelets, and sphere.

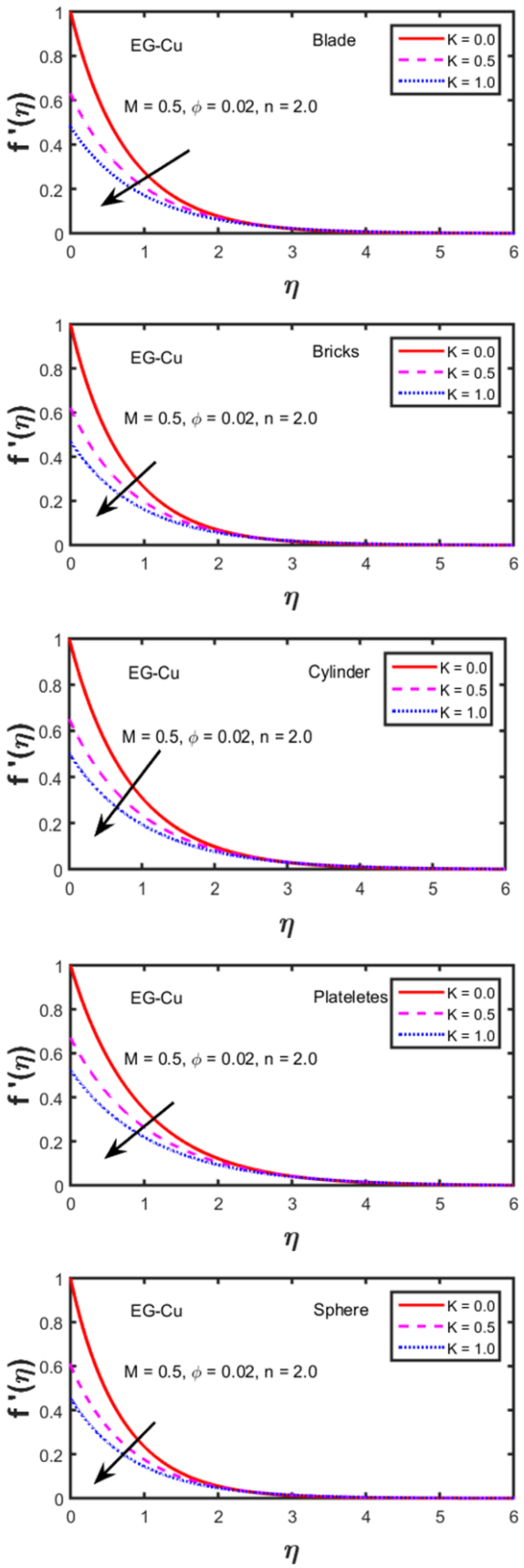

Fig. 4. Impact of slip parameter (K) on the velocity profile of EG-Cu nanofluid for various nanoparticle shapes: blade, brick, cylinder, platelets, and sphere.

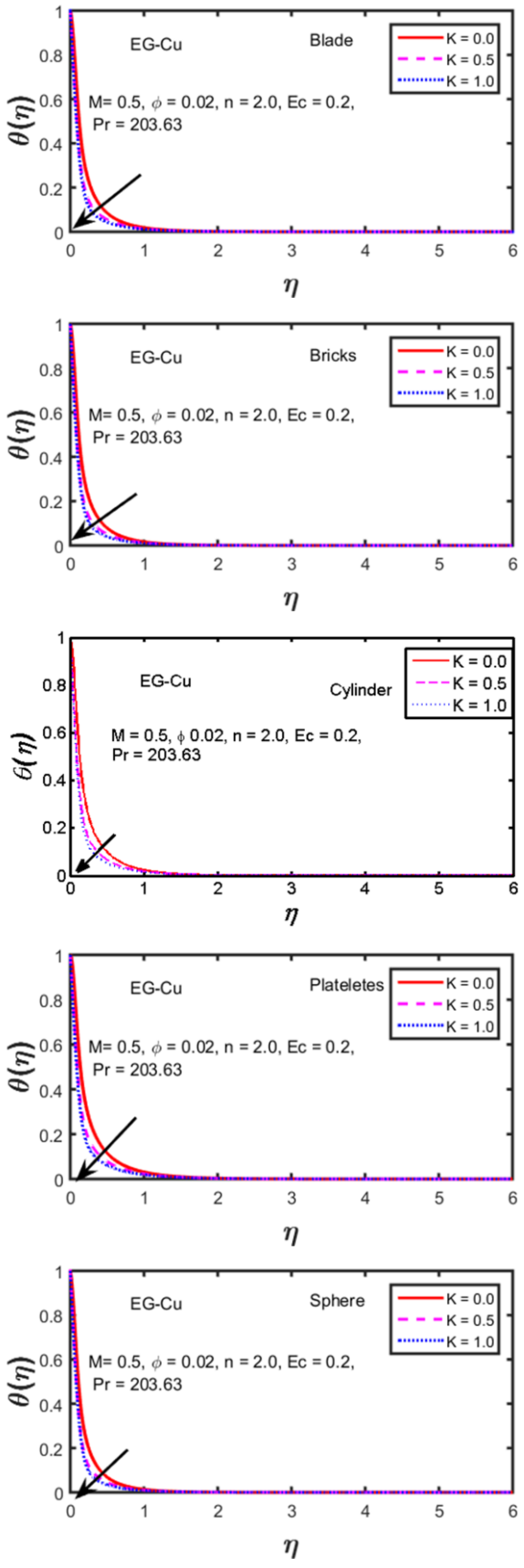

Fig. 5. Impact of the slip parameter (K) on the temperature profile of EG-Cu nanofluid for various nanoparticle shapes: blade, brick, cylinder, platelets, and sphere.

Increasing the slip parameter K reduces the friction at the boundary, which in turn reduces the rate of convective heat transfer. This reduction in heat transfer efficiency leads to a decrease in the temperature distribution within the EG-Cu nanofluid, regardless of the nanoparticle shape (blade, brick, cylinder, platelets, or sphere). Different shapes will exhibit different magnitudes of this effect due to their varying thermal conductivity and interaction with the base fluid, but the overall trend with respect to *K* will be the same.

Figure 6 demonstrates the influence of the nanoparticle volume fraction (ϕ) on the velocity profile for EG-Cu nanofluid for five nanoparticle shapes: blade, brick, cylinder, platelets, and sphere. The results demonstrate how the concentration of nanoparticles affects fluid flow, with each shape exhibiting unique flow characteristics. For instance, blade-shaped nanoparticles, with their sharp and elongated design, tend to increase resistance and turbulence, causing noticeable changes in the velocity profile. In contrast, spherical particles, due to their smooth and symmetrical shape, enable more uniform and stable flow. Platelet-shaped particles, with their flat and wide structure, enhance the velocity profile, while cylindrical and brick-shaped particles show intermediate flow patterns. Notably, increasing ϕ enhances the velocity for most copper nanoparticle shapes, including cylinders, platelets, blades, and bricks. However, a unique exception is observed for spherical nanoparticles, where increasing ϕ leads to a velocity decrease. This contrasting behaviour can be attributed to the interplay between various factors such as particle shape, interparticle interactions, and heat transfer mechanisms. Figure 7 delves into the influence of nanoparticle volume fraction (ϕ) on the temperature for EG-Cu nanofluid for various nanoparticle shapes. The results are presented for blade, brick, cylinder, platelets, and sphere, highlighting the influence of shape factor on the temperature profile. Interestingly, increasing ϕ generally leads to a temperature increase for most copper nanoparticle shapes, including cylinders, platelets, blades, and bricks. This can be attributed to enhanced heat generation within the nanofluid due to higher particle concentration.

The impact of the stretching parameter (n) on the velocity profile with different shapes of copper nanoparticles is shown in Fig. 8 for the EG-Cu nanofluid for five nanoparticle shapes: blade, brick, cylinder, platelets, and sphere. The results demonstrate how the rate of surface stretching influences fluid flow, with each nanoparticle shape showing unique flow characteristics. These findings highlight the significant role of nanoparticle geometry in determining fluid dynamics during stretching, providing critical insights for applications, such as industrial coating, polymer processing, or flexible electronics, where controlling flow behaviour under deformation is essential for optimizing performance. The velocity profile also tends to reduce with a rise in n values, as mentioned earlier; a rise in the values of n reduces the boundary layer thickness.

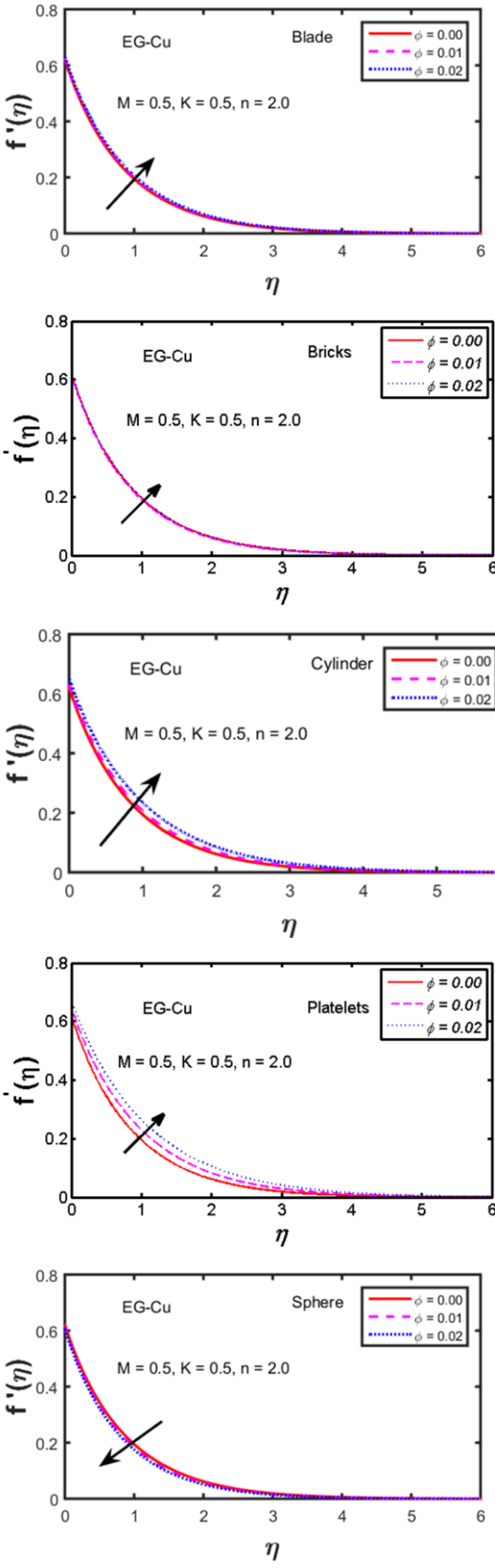

Fig. 6. Impact of volume fraction (ϕ) on the velocity profile of EG-Cu nanofluid for various nanoparticle shapes: blade, brick, cylinder, platelets, and sphere.

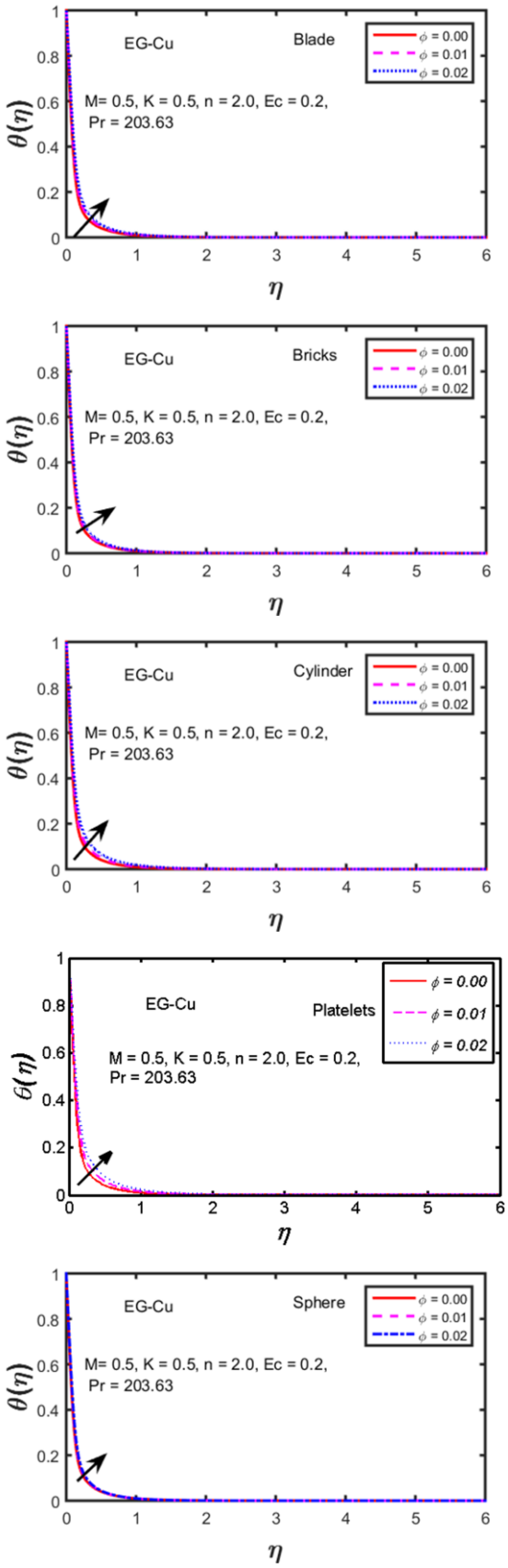

Fig. 7. Impact of volume friction (ϕ) on the temperature profile of EG-Cu nanofluid for various nanoparticle shapes: blade, brick, cylinder, platelets, and sphere.

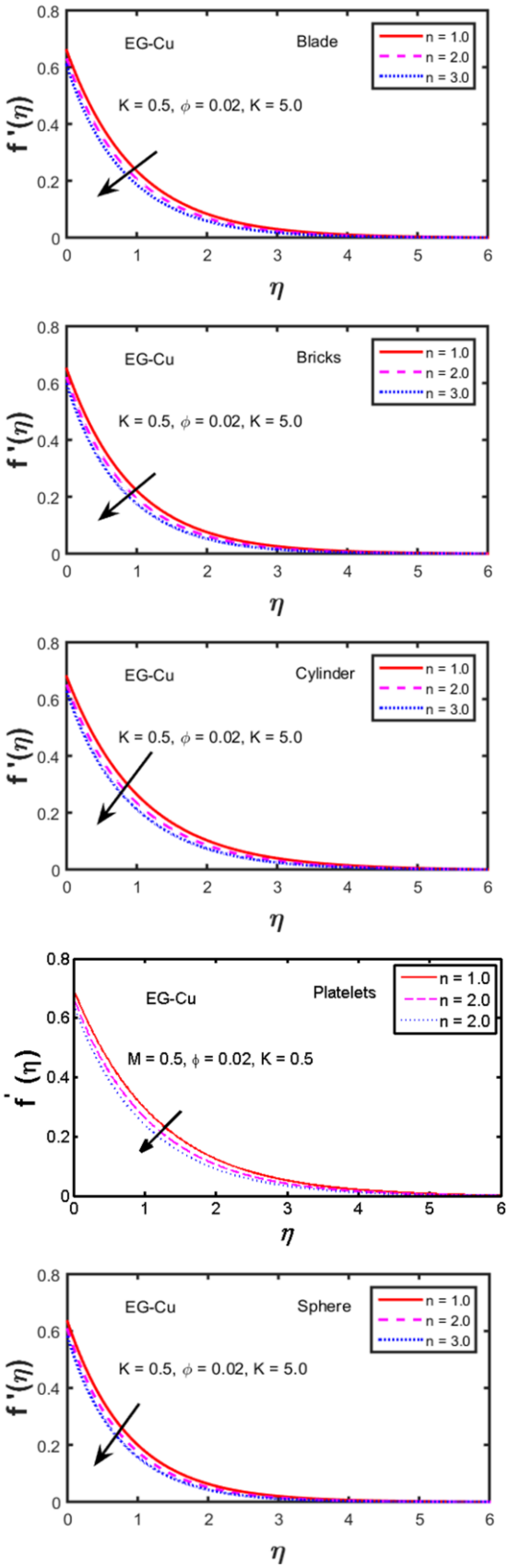

Fig. 8. Effect of the stretching parameter (n) on the velocity profile of EG-Cu nanofluid for various nanoparticle shapes: blade, brick, cylinder, platelets, and sphere.

Figure 9 portrays the impact of stretching parameter (n) on the temperature profile for EG-Cu nanofluid for five nanoparticle shapes: blade, brick, cylinder, platelets, and sphere. The results illustrate how the rate of surface stretching influences thermal behaviour, with each nanoparticle shape displaying distinct heat transfer characteristics.

The findings emphasize the importance of optimizing nanoparticle shape to achieve desired thermal performance in systems, where stretching and heat transfer are interconnected. It is noted that the temperature also reduces with a rise in the stretching parameter.

Figure 10 sheds light on the role of the Eckert number (Ec) in shaping the temperature profile. As Ec increases, we observe a further enhancement in temperature. This signifies the growing importance of viscous dissipation with increasing fluid velocity.

Figure 11 provides an intriguing comparison of the velocity profiles for different copper nanoparticle shapes. We observe that the velocity ranking, from highest to lowest, is as follows: platelets, cylinders, blades, bricks and spheres. This suggests that platelet-shaped nanoparticles offer the strongest enhancement in nanofluid velocity, while spherical nanoparticles exhibit the least impact.

Finally, Fig. 12 offers a scientifically compelling results for comparison of temperature profiles for different copper nanoparticle shapes. We can discern that the temperature ranking, from highest to lowest, follows the order: platelets, cylinders, blades, bricks and spheres. This suggests that platelet-shaped nanoparticles have the most significant impact on heat generation, while spherical nanoparticles contribute the least. These findings unveil the intricate relationships between various parameters and their impact on the thermal behaviour of copper nanofluids. Such insights can guide the design and optimization of nanofluid-based systems for diverse applications in thermal management, energy harvesting, and beyond.

Table 1 shows the physical and thermal characteristics of base fluids and copper nanoparticles [32] and Table 2 exhibits the varying values of the shape factor and viscosity of fluid under consideration [31]. In Table 3, the current result is contrasted with the findings of Khan and Pop [47], Wang [48], and Reddy Gorla and Sidawi [49] across a range of Prandtl numbers. We noticed that our results are in great agreement with existing literature for specific values. In Table 4, numerical values of skin friction are listed for different shapes of copper nanoparticles under various physical conditions. The data show that an increase in volume fraction (ϕ), magnetic field strength (M) and stretching parameter (n) leads to an increase in the skin friction coefficient for multi-shaped copper nanoparticles. However, the trend is reversed for the slip parameter (K). In Table 5, the heat transfer coefficient (Nusselt number, Nu) is computed for parameters such as magnetic field strength (M), volume fraction (ϕ) stretching parameter (n) and slip parameter (K). The Nusselt number reduces with increasing values of magnetic field strength (M), volume fraction (ϕ) and Eckert number (Ec), for multi-shaped copper nanoparticles. Conversely, a different pattern is observed for the slip parameter (K) and stretching parameter (n).

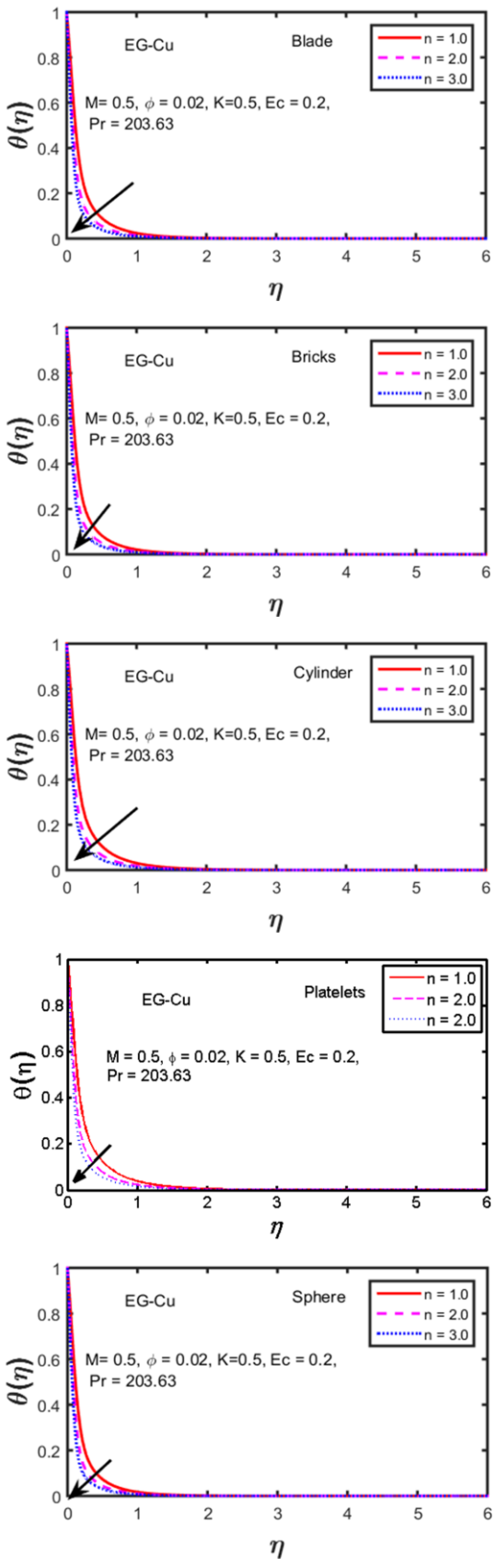

Fig. 9. Effect of the stretching parameter (n) on the temperature profile of EG-Cu nanofluid for various nanoparticle shapes: blade, brick, cylinder, platelets, and sphere.

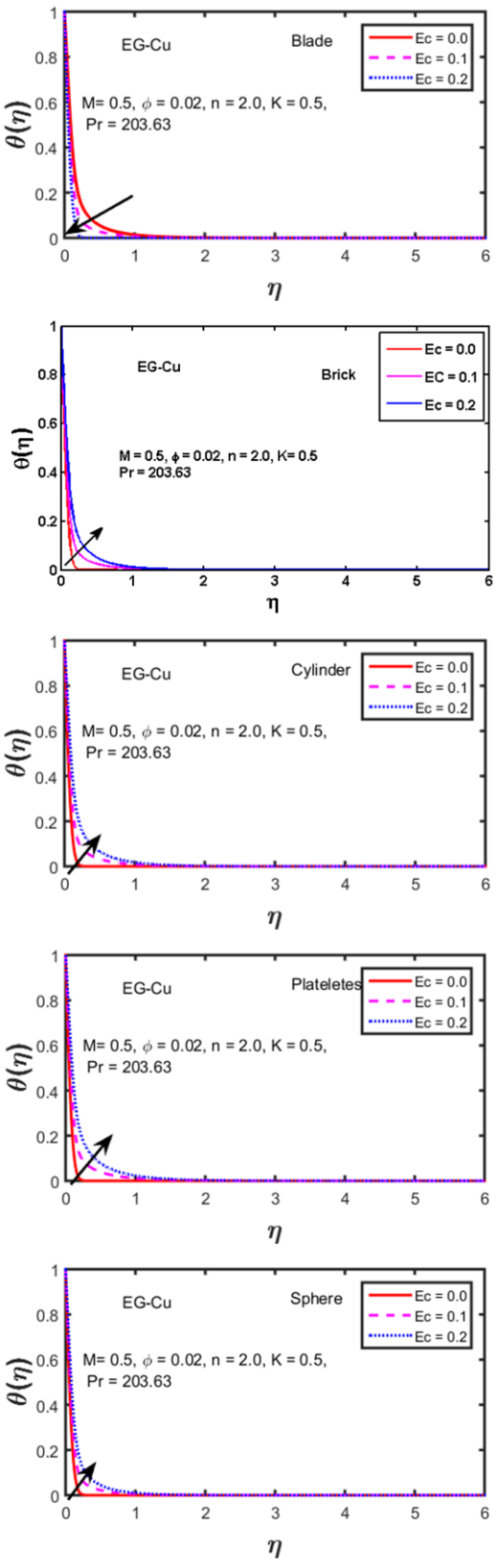

Fig. 10. Impact of the Eckert number (Ec) on the temperature profile of EG-Cu nanofluid for various nanoparticle shapes: blade, brick, cylinder, platelets, sphere.

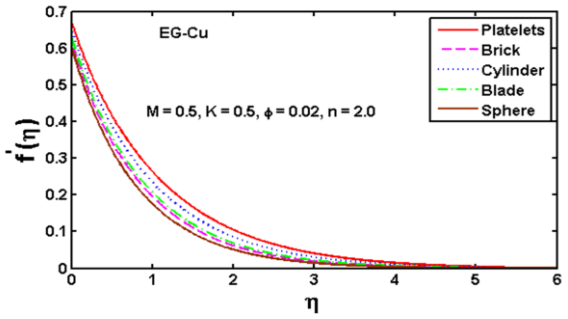

Fig 11. Impact of nanoparticle shape on the velocity profile.

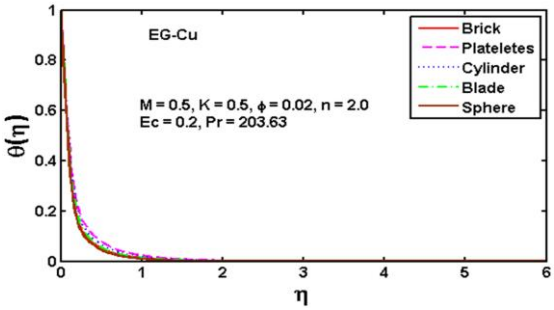

Fig. 12: Impact of nanoparticle shape on the temperature profile.

Table 1. Physical and thermal characteristics of base fluids and copper nanoparticles [32].

Nanoparticles / Base fluid	Specific heat, C_p (J/kgK)	Thermal conductivity, k (W/m K)	Density, ρ (kg/m^3)
Copper	385	401.0	8933
Ethylene glycol	2430	0.253	1115

Table 2. Varying values of the shape factor and viscosity [31].

Parameters / Nanoparticles	A_1	A_2	m
Blade	14.6	123.3	8.26
Brick	1.0	471.4	3.72
Cylinder	13.5	904.4	4.82
Platelets	37.1	612.6	5.72
Sphere	2.5	6.5	3.00

Table 3. Comparison of results for the reduced Nusselt number $\theta'(0)$ considering: $K = 0,\ M = 0,\ \phi = 0,\ \mathrm{Ec} = 0,\ n = 1.$

Pr	Khan [1]	Wang [2]	Sidawi [50]	Present
0.7	0.4539	0.4539	0.53	0.4544
2.0	0.9113	0.9114	0.9114	0.9114
7.0	1.8954	1.8954	1.8905	1.8954
20.0	3.3539	3.3539	3.3539	3.3539
70.0	6.4621	6.4622	6.4622	6.4622

Table 4. Values of skin-friction coefficient for multi-shape nanoparticles.

M	K	ϕ	n	$C_f\mathrm{Re}^{\frac{1}{2}}$				
				Cylinder	Platelets	Sphere	Blade	Brick
0.5	0.5	0.02	2	-1.138160	-1.306940	-0.830585	-0.989867	-0.928154
0.0	–	–	–	-0.998848	-1.145640	-0.731201	-0.869857	-0.816152
1.0	–	–	–	-1.246380	-1.433560	-0.906007	-1.082130	-1.013850
.5	0.0	–	–	-2.023270	-2.232800	-1.624970	-1.834350	-1.754120
–	1.0	–	–	-0.811870	-0.945852	-0.573870	-0.696044	-0.648416
–	0.5	0.00	–	-0.758920	-0.758920	-0.758920	-0.758920	-0.758920
–	–	0.01	–	-0.903964	-1.010440	-0.794841	-0.868059	-0.817518
–	–	0.02	1	-1.046630	-1.197250	-0.770443	-0.913785	-0.858335
–	–	–	3	-1.210200	-1.393640	-0.877531	-1.049520	-0.982801

Table 5: Comparison of the numerical values of Nusselt number for multi-shape nanoparticles.

M	K	Ec	ϕ	n	$\mathrm{NuRe}^{-\frac{1}{2}}$				
					Cylinder	Platelets	Sphere	Blade	Brick
0.5	0.5	0.2	0.02	2	5.797680	5.45369	6.40553	6.41026	6.22636
0.0	–	–	–	–	8.654940	8.54567	8.79801	9.11713	8.77341
1.0	–	–	–	–	3.635770	3.07073	4.66863	4.40239	4.3504
0.5	0.0	–	–	–	0.340441	−0.13803	1.35575	1.03829	1.0155
–	1.0	–	–	–	6.716180	6.57152	6.89114	7.12693	6.8602
–	0.5	0.0	–	–	11.574800	11.8706	10.91440	11.7129	11.1567
–	–	0.1	–	–	8.686250	8.66215	8.65996	9.06153	8.69152
–	–	0.2	0.00	–	6.892040	6.89204	6.89204	6.89204	6.89204
–	–	–	0.01	–	6.472940	6.26860	6.64252	6.68574	6.62141
–	–	–	0.02	1	3.334780	2.91268	4.12472	3.94395	3.87874
–	–	–		3	7.679450	7.39147	8.15487	8.29984	8.02463

5. Conclusions

In this article, heat transfer enhancement due to variation in copper nanoparticle shape factor for blades, spheres, bricks, cylinders and platelets in a nanofluid over stretching surfaces has been studied theoretically. Additionally, the effect of thermophysical quantities like volume fraction on heat transfer rates has been investigated. It is observed in this study that the surface area of nanoparticles greatly influences the thermal conductivity and all other properties of the nanofluid, and the increase in shape factor values enhances the heat transfer rate. Hence, the heat transfer rate for bricks is the highest in comparison to all other shapes of nanoparticles due to the large interfacial contact area. Regarding the role of the shape factors in heat transfer, it has been concluded that brick-shaped nanoparticles can be considered a good choice for future nanofluid applications in heat exchangers.

Based on the obtained results, the new findings are as follows:

- Nanoparticles in the shape of platelets offer excellent flow and bricks offer excellent heat transfer properties.
- Spherical nanoparticles have poor flow and heat transfer rates as compared to other shapes.
- An increase in the magnetic parameter M reduces velocity and hence decreases the boundary layer thickness.
- The interaction of the magnetic field and the conducting fluid causes Joule heating, which occurs when electrical energy is transformed into heat by flow-induced currents. This increased heat generation influences the temperature distribution and results in an increase in temperature.
- Increasing the slip parameter reduces both velocity and temperature profiles.
- Increasing the stretching parameter value reduces both the velocity distribution and the temperature of the copper nanofluid.
- An increase in the volume fraction enhances velocity and temperature profiles.
- Nusselt number enhances with increasing values of all parameters, such as the slip parameter and stretching parameter.
- Comparing the impact of the Eckert number, volume fraction and magnetic parameter, it was found that the Nusselt number decreases as these parameters increase.
- Skin fraction magnitude increases for increasing values of volume fraction, stretching parameter, and magnetic parameter, and decreases for increasing values of slip parameter.

References

[1] Eastman, J.A., Choi, S.U.S., Li, S., Yu, W., & Thompson, L.J. (2001). Anomalously increased effective thermal conductivities of ethylene glycol-based nanofluids containing copper nanoparticles. *Applied Physics Letters*, 78(6), 718−720. doi: 10.1063/1.1341218

[2] Chakraborty, S., & Panigrahi, P.K. (2020). Stability of nanofluid: A review. *Applied Thermal Engineering*, 74, 115259. doi: 10.1016/j.applthermaleng.2020.115259

[3] Patel, H.E., Das, S.K., Sundararajan, T., Sreekumaran Nair, A., George, B., & Pradeep, T. (2003). Thermal conductivities of naked and monolayer protected metal nanoparticle based nanofluids: Manifestation of anomalous enhancement and chemical effects. *Applied Physics Letters*, 83(14), 2931−2933. doi: 10.1063/1.1602578

[4] Liu, I.C., Wang, H.H., & Liu, C.N. (2013). Flow and heat transfer of nanofluids near a rotating disk. *Advanced Materials Research*, 664, 859−865. doi: 10.4028/www.scientific.net/AMR.664.859

[5] Das, K. (2014). Flow and heat transfer characteristics of nanofluids in a rotating frame. *Alexandria Engineering Journal*, 53(3), 757−766. doi: 10.1016/j.aej.2014.04.003

[6] Pandey, A.K., & Upreti, H. (2023). Heat and mass transfer in convective flow of nanofluid. In *Advances in Mathematical and Computational Modeling of Engineering Systems* (pp. 295−313). CRC Press. doi: 10.1201/9781003367420-14

[7] Srisailam, B., Reddy, K.S., Narender, G., & Malga, B.S. (2022). Flow and heat transfer analysis of MHD nanofluid due to convective stretching sheet. *Indian Journal of Science and Technology*, 15(44), 2393−2402. doi: 10.17485/ijst/v15i44.1006

[8] Sakiadis, B.C. (1961). Boundary-layer behavior on continuous solid surfaces: II. The boundary layer on a continuous flat surface. *AIChE Journal*, 7(2), 221−225. doi: 10.1002/aic.690070211

[9] Ferdows, M., Ramesh, G.K., & Madhukesh, J.K. (2023). Magnetohydrodynamic flow and Hall current effects on a boundary layer flow and heat transfer over a three-dimensional stretching surface. *International Journal of Ambient Energy*, 44(1), 938−946. doi: 10.1080/01430750.2022.2157873

[10] Ahmad, B., Abbas, T., Fatima, K., Duraihem, F.Z., & Saleem, S. (2024). Nonlinear flow of hybrid nanofluid with thermal radiation: A numerical investigation. *ZAMM Journal of Applied Mathematics and Mechanics*, 104(1), e202200170. doi: 10.1002/zamm.202200170

[11] Eid, M.R., Mahny, K.L., Muhammad, T., & Sheikholeslami, M. (2018). Numerical treatment for Carreau nanofluid flow over a porous nonlinear stretching surface. *Results in Physics*, 8, 1185−1193. doi: 10.1016/j.rinp.2018.01.070

[12] Hayat, T., Saif, R.S., Ellahi, R., Muhammad, T., & Ahmad, B. (2017). Numerical study of boundary-layer flow due to a nonlinear curved stretching sheet with convective heat and mass conditions. *Results in Physics*, 7, 2601−2606. doi: 10.1016/j.rinp.2017.07.023

[13] Zaimi, K., Ishak, A., & Pop, I. (2014). Boundary layer flow and heat transfer over a nonlinearly permeable stretching/shrinking sheet in a nanofluid. *Scientific Reports*, 4, 4404. doi: 10.1038/srep04404

[14] Athar, M., Ahmad, A., & Khan, Y. (2023). Polymer presence in boundary layer flow and heat transfer of dusty fluid over a stretching surface. *Multidiscipline Modeling in Materials and Structures*, 19(4), 617−633. doi: 10.1108/mmms-09-2022-0167

[15] Shah, G., Rehman, A., & Sheikh, N. (2022). Heat transfer analysis over the boundary layer stagnation-point flow of couple stress fluid over an exponentially stretching sheet. *American Journal of Applied Mathematics*, 10(3), 100−105. doi: 10.11648/j.ajam.20221003.13

[16] Venkateswarlu, S., Varma, S., & Kumar, R.K. (2022). Boundary layer flow of a conducting hyperbolic nanofluid over a stretching surface with chemical reaction and heat source/sink. *Journal of Theoretical and Applied Mechanics*, 52(2), 179–196. doi: 10.55787/jtams.22.52.2.179

[17] Vidhya, M., Juliet, S.S., Govindarajan, A., & Priyadarshini, E. (2022). An axisymmetric flow over non-linear radially stretching surface with heat transfer and chemical reaction effects. *AIP Conference Proceedings*, 2516(1), 170027. doi: 10.1063/5.0108677

[18] Hashim, H., Sarif, N.M., Salleh, M.Z., & Mohamed, M.K.A. (2020). Aligned magnetic field on Williamson fluid over a stretching sheet with Newtonian heating. *Journal of Physics: Conference Series*, 1529, 052085. doi: 10.1088/1742-6596/1529/5/052085

[19] Chen, C.H. (2010). Combined effects of Joule heating and viscous dissipation on magnetohydrodynamic flow past a permeable, stretching surface with free convection and radiative heat transfer. *Journal of Heat Transfer*, 132(6), 064503. doi: 10.1115/1.4000946

[20] Khashi'ie, N.S., Arifin, N.M., Pop, I., & Wahid, N.S. (2020). Flow and heat transfer of hybrid nanofluid over a permeable shrinking cylinder with Joule heating: A comparative analysis. *Alexandria Engineering Journal*, 59(3), 1787−1798. doi: 10.1016/j.aej.2020.04.048

[21] Srinivasacharya, D., & Jagadeeshwar, P. (2019). Effect of Joule heating on the flow over an exponentially stretching sheet with convective thermal condition. *Mathematical Sciences*, 13(3), 201−211. doi: 10.1007/s40096-019-0290-8

[22] Ganesh Kumar, K., Rudraswamy, N.G., Gireesha, B.J., & Krishnamurthy, M.R. (2017). Influence of nonlinear thermal radiation and viscous dissipation on three-dimensional flow of Jeffrey nano fluid over a stretching sheet in the presence of Joule heating. *Nonlinear Engineering*, 6(3), 207−219. doi: 10.1515/nleng-2017-0014

[23] Ghaffarpasand, O. (2016). Numerical study of MHD natural convection inside a sinusoidally heated lid-driven cavity filled with FeO-water nanofluid in the presence of Joule heating. *Applied Mathematical Modelling*, 40(21-22), 9165–9182. doi: 10.1016/j.apm.2016.05.038

[24] Mutuku, W.N., Makinde, O.D., & Theuri, D. (2017). Hydromagnetic mixed convection flow of nanofluid with slip, viscous dissipation and Joule heating past an inclined plate. *Journal of Nanofluids*, 6(6), 1065−1073. doi: 10.1166/jon.2017.1404

[25] Ali, B., Jubair, S., Al-Essa, L. A., Mahmood, Z., Al-Bossly, A., & Alduais, F.S. (2023). Boundary layer and heat transfer analysis of mixed convective nanofluid flow capturing the aspects of nanoparticles over a needle. *Materials Today Communications*, 35, 106253. doi: 10.1016/j.mtcomm.2023.106253

[26] Shankar Goud, B., Dharmendar Reddy, Y., & Mishra, S. (2023). Joule heating and thermal radiation impact on MHD boundary layer Nanofluid flow along an exponentially stretching surface with thermal stratified medium. *Proceedings of the Institution of Mechanical Engineers, Part N: Journal of Nanomaterials, Nanoengineering and NanoSystems*, 237(3-4), 107−119. doi: 10.1177/23977914221100961

[27] Khashi'ie, N.S., Arifin, N.M., & Pop, I. (2022). Magnetohydrodynamics (MHD) boundary layer flow of hybrid nanofluid over a moving plate with Joule heating. *Alexandria Engineering Journal*, 61(3), 1938−1945. doi: 10.1016/j.aej.2021.07.032

[28] Rana, P., Mahanthesh, B., Nisar, K. S., Swain, K., & Devi, M. (2021). Boundary layer flow of magneto-nanomicropolar liquid over an exponentially elongated porous plate with Joule heating and viscous heating: a numerical study. *Arabian Journal for Science and Engineering*, 46, 12405−12415. doi: 10.1007/s13369-021-05926-8

[29] Tarakaramu, N., Satya Narayana, P.V., Babu, D.H., Sarojamma, G., & Makinde, O.D. (2021). Joule Heating and dissipation effects on magnetohydrodynamic couple stress nanofluid flow over a bidirectional stretching surface. *International Journal of Heat and Technology*, 39(1), 205−212. doi: 10.18280/ijht.390122

[30] Saleem, S., Qasim, M., Alderremy, A., & Noreen, S. (2020). Heat transfer enhancement using different shapes of Cu nanoparticles in the flow of water based nanofluid. *Physica Scripta*, 95(5), 055209. doi: 10.1088/1402-4896/ab4ffd

[31] Fakour, M., Rahbari, A., Khodabandeh, E., & Ganji, D.D. (2018). Nanofluid thin film flow and heat transfer over an unsteady stretching elastic sheet by LSM. *Journal of Mechanical Science and Technology*, 32, 177−183. doi: 10.1007/s12206-017-1219-5

[32] Mathews, J., & Tallab, H. (2024). Unsteady magnetohydrodynamic free convection and heat transfer flow of Al_2O_3-Cu/water nanofluid over a non-linear stretching sheet in a porous medium. *Archives of Thermodynamics*, 45(3), 165–173. doi: 10.24425/ather.2024.150449

[33] Triveni, B., Rao, M.V.S., Gangadhar, K., & Chamkha, A.J. (2024). Heat transfer analysis of MHD Casson nanofluid flow over a nonlinear stretching sheet in the presence of nonuniform heat source. *Numerical Heat Transfer, Part A: Applications*, 85(13), 2145−2164. doi: 10.1080/10407782.2023.2219831

[34] Hayat, U., Ali, R., Shaiq, S., & Shahzad, A. (2023). A numerical study on thin film flow and heat transfer enhancement for copper nanoparticles dispersed in ethylene glycol. *Reviews on Advanced Materials Science*, 62(1), 20220320. doi: 10.1515/rams-2022-0320

[35] Sathyanarayana, M., & Goud, T.R. (2023). Numerical study of MHD Williamson-nano fluid flow past a vertical cone in the presence of suction/injection and convective boundary conditions. *Archives of Thermodynamics*, 44(2), 115−138. doi: 10.24425/ather.2023.146561

[36] Joachimiak, D., Judt, W., & Joachimiak, M. (2023). Numerical analysis of the heating of a die for the extrusion of aluminium alloy profiles in terms of thermochemical treatment. *Archives of Thermodynamics*, 44(2), 159−175. doi: 10.24425/ather.2023.146563

[37] Hayat, U., & Shahzad, A. (2023). Thin film flow, heat transfer and viscous dissipation effects on vertical stretching sheet for different shapes of (Au-Np) dispersed in water. *Physica Scripta*, 98(10), 105251. doi: 10.1088/1402-4896/acfb4e

[38] Hayat, U., & Shahzad, A. (2023). Analysis of heat transfer and thin film flow of Au-Np over an unsteady radial stretching sheet. *Numerical Heat Transfer, Part A: Applications*, 84(11), 1338−1351. doi: 10.1080/10407782.2023.2175746

[39] Ali, R., Iqbal, A., Abbass, T., Arshad, T., & Shahzad, A. (2024). Unsteady flow of silica nanofluid over a stretching cylinder with effects of different shapes of nanoparticles and Joule heating. *Archives of Thermodynamics*, 45(3), 115–126. doi: 10.24425/ather.2024.151222

[40] Gangadhar, K., Naga Chandrika, G., & Dinarvand, S. (2025). Investigation into silver-engine oil nanoliquid convinced by Riga surface: Deviations in three binary nanofluids. *Modern Physics Letters B*, 39(01), 2450385. doi: 10.1142/s0217984924503858

[41] Gangadhar, K., Vardhana, K.A., & Wakif, A. (2024). HVAC-solar energy performance exploiting Sutterby (AA7075–Ag–Cu/$C_6H_9NaO_7$) ternary magnetic nanofluid through spinning flow with joule heating. *Modern Physics Letters B*, 39(14), 2450493. doi: 10.1142/S0217984924504931

[42] Gangadhar, K., Sangeetha Rani, M., & Wakif, A. (2024). Non-Fourier heat flux and Joule dissipation in hybrid nanoparticles suspension with Williamson fluid. *The European Physical Journal Plus*, 139, 306. doi: 10.1140/epjp/s13360-024-05054-w

[43] Gangadhar, K., Sree, T. S., Wakif, A., & Subbarao, K. (2024). Stefan blowing impact and chemical response of Rivlin-Reiner fluid through rotating convective disk. *Pramana Journal of Physics*, 98, 160. doi: 10.1007/s12043-024-02836-w

[44] Gangadhar, K., Rao, M.V.S., Kumari, M.A., & Wakif, A. (2024). Impact of the Stefan gusting on a bioconvective nanofluid with the various slips over a rotating disc and a substance-responsive specie. *Modern Physics Letters B*, 39(1), 2450406. doi: 10.1142/s0217984924504062

[45] Gangadhar, K., Sujana Sree, T., & Wakif, A. (2024). Generalized slip impact of Casson nanofluid through cylinder implanted in swimming gyrotactic microorganisms. *International Journal of Modern Physics B*, 38(28), 2450380. doi: 10.1142/s0217979224503806

[46] Gangadhar, K., Rani, M.S., & Wakif, A. (2024). Ternary nanofluids due to moving wedge with strong magnetic field and convective condition. *International Journal of Modern Physics B*, 39(03), 2550026. doi: 10.1142/s0217979225500262

[47] Khan, W.A., & Pop, I. (2010). Boundary-layer flow of a nanofluid past a stretching sheet. *International Journal of Heat and Mass Transfer*, 53(11-12), 2477–2483. doi: 10.1016/j.ijheatmasstransfer.2010.01.032

[48] Wang, C.Y. (1989). Free convection on a vertical stretching surface. *ZAMM Journal of Applied Mathematics and Mechanics*, 69(11), 418–420. doi: 10.1002/zamm.19890691115

[49] Reddy Gorla, R.S., & Sidawi, I. (1994). Free convection on a vertical stretching surface with suction and blowing. *Applied Scientific Research*, 52, 247–257. doi: 10.1007/bf00853952